Mapping of crystal surfaces onto the five-vertex model

M. Gulácsi
Theoretical Division, Los Alamos National Laboratory, Los Alamos, New Mexico 87545

A. C. Levi
Università di Genova, Dipartimento di Fisica, 16146 Genova, Italy

E. Tosatti
Scuola Internazionale Superiore di Studi Avanzati, Via Beirut 4, Miramare, 34014 Trieste, Italy
and International Centre for Theoretical Physics, P.O.Box 586, 34014 Trieste, Italy
(Received 14 December 1993)

Within the solid-on-solid framework we map certain surfaces of a simple cubic crystal onto a five-vertex model. The mapping scheme used differs from the more common body-centered solid-on-solid mapping, which uses a six-vertex model and is only suitable for interfaces whose lattice splits naturally into two sublattices. In the five-vertex model there is no touching of step lines and the arrow-reversal symmetry is broken by construction. After reviewing the exact solution of the five-vertex model and studying its phase diagram in the presence of an external field, we establish an isomorphism between some phases of the vertex model with the (100), (110) and $(\bar{1}01)$ faces of the simple cubic crystal. We determine exactly the mean square height difference. If no *field* is applied the flat surfaces undergo a transition at a critical temperature, where the inclination of the surfaces begins to change, and roughening sets in. If, however, the inclination is kept constant by applying a suitable field, the low-index flat (or high-index vicinal) surfaces remain smooth (or rough) from zero up to infinite temperature, without undergoing any roughening transition.

PACS number(s): 05.50.+q

I. INTRODUCTION

The most frequently used model for a crystal-vapor interface is the solid-on-solid (SOS) model [1]. The atoms are densely packed in a lattice; at the interface the atoms may sit on top of each other, but overhangs and vacancies are excluded. Since there is no vapor, and also since the bulk of the so-defined SOS crystal does not contribute any degrees of freedom to the system and does not melt, the model merely describes the solid surface in a simplified strictly two-dimensional form. The first argument for the existence of a singularity in the free energy of this system was given in Ref. [1]: for the crystal this means [2] that above this singularity the surface is rough, i.e., the nucleation barrier for two-dimensional nucleation vanishes. It is well known that some versions of the SOS model, which correspond to certain surfaces of well-defined crystals, are isomorphic [3–5] to exactly solvable vertex models, in particular to the six-vertex model [6,7]. This mapping scheme, proposed by van Beijeren [3], is suitable for lattices which can be divided naturally into two sublattices, i.e., bipartite lattices, as is the case of (100) surfaces of bcc [3], or (100) and (110) of fcc [4,5] crystals. (We will use here the word *bipartite* in a somewhat more restricted sense than elsewhere in the literature, requiring not only that the lattice *can* be split into two sublattices, but also that such splitting occurs *naturally*.) For nonbipartite lattices, such as, e.g., the simple cubic (sc) crystal, however, this is not the case. In order to describe nonbipartite crystal surfaces exhibiting square or rectangular symmetry another mapping procedure must be used.

Such a new method was introduced recently by Garrod, Levi, and Touzani [8] (GLT) (as a natural extension of previous studies by Garrod on two-dimensional growth models [9]). For simplicity, we will treat here the surfaces of a sc crystal. Since this mapping scheme is still relatively new, we shall briefly review it, before proceeding on.

Following closely Ref. [8], let us consider a rectangular $N_0 \times M_0$ table, where a discrete height variable m_{ij} is defined at every site (ij). Let there be L_0 steps (monatomic or not) running obliquely from bottom left to top right, and let L be the total level difference between the upper and lower ends of the right side of the table. Thus, if s labels the steps and if the sth step corresponds to a jump of Δm_s units, then $L = \sum_s \Delta m_s$. On the average the y coordinate of each step changes by $\Delta y = S$ from the left to the right end of the table. Then the Miller indices (hkl) of the vicinal surface so defined $(h < 0; k, l > 0)$ obey the relation $|h|/k = S/N_0$ and $k/l = L/M_0$.

If multiple steps exist, a sliding procedure can be applied [8] to split them into single steps, so that we can consider single steps only on the crystal surface. The number of steps now becomes $L > L_0$. The size of the table (originally $N_0 \times M_0$) is now changed. We assume that N_0 and M_0 had been chosen so that the resulting table is now a square of side N, with $N \leq N_0, M_0$. We have $M_0 = N - L$, $N_0 = N - Q$, where $Q = LS/N$. Thus the Miller indices are given by $h = -Q/u$, $k = L/u$, and

$l = (N-L)/u$, where u is the largest common factor of Q, L, and $N-L$. The steps so formed can now be identified with the lines of the *line representation* of the six-vertex model [7]. However, by virtue of the sliding procedure described above, no touching of lines will occur at any site. Vertex 2 (in the usual notation for vertices) is actually absent and we are left with a five-vertex model. Thus the nonbipartite crystal surfaces possessing square or rectangular symmetry are isomorphic to the five-vertex model, in contrast to the bipartite surfaces, which are isomorphic to the six-vertex model. Three-point correlations, very important for the GLT growth model, have been calculated in an elegant paper by Garrod [10]. In a previous publication [11] we have presented the exact solution of the five-vertex model on a square lattice. In the following we will briefly review the main results.

On each link a variable taking two values (the *arrow*) is defined; four crossing links form a *vertex*. To each vertex a Boltzmann weight $\omega_i = \exp(-\beta\varepsilon_i)$ is associated, ε_i being the vertex energy. The most general such model is referred to as the sixteen($= 2^4$)-vertex model (unsolved).

Choosing the Boltzmann weights so that only the six vertices with two entering and two exiting arrows have finite weight, we have the usual six-vertex model [6,7]. In this case there are only four independent energies to consider. This is because (a) the zero of energy can be chosen arbitrarily and (b) the ice rule implies that $\varepsilon_5 = \varepsilon_6$ is no restriction, since vertices 5 and 6 always occur in pairs.

Similarly, the field-free five-vertex case is defined [11] by three Boltzmann weights (reducing further to two independent parameters when the arbitrariness of the zero of energy is taken into account), i.e., $\omega_1 \equiv \exp(-\beta\varepsilon_1)$, $\omega_3 \equiv \exp(-\beta\varepsilon_3) = \omega_4 \equiv \exp(-\beta\varepsilon_4)$, and $\omega_5 \equiv \exp(-\beta\varepsilon_5) = \omega_6 \equiv \exp(-\beta\varepsilon_6)$. Using these conditions and applying the Bethe ansatz afresh [12] the general five-vertex model was solved [11,13]. In terms of the variables $x = \omega_1/\omega_5$ and $y = \omega_3/\omega_5$ the free energy is

$$f_L = \min_{p_v} \left\{ \varepsilon_1 - k_B T \int_{-Q^*}^{+Q} \ln\left(\frac{1-\Delta_5 e^{ip}}{x/y - e^{ip}}\right) \rho(p)dp \right\} , \tag{1}$$

where the interaction constant of the five-vertex model Δ_5 is defined as $\Delta_5 = (\omega_3^2 - \omega_5^2)/\omega_1\omega_3$, the distribution function is here simply

$$\rho(p) = \frac{1}{2\pi}\left[1 + \frac{1-p_v}{2}\frac{\Delta_5 e^{ip}}{1-\Delta_5 e^{ip}}\right] , \tag{2}$$

and p_v is the vertical polarization $p_v = (n_1+n_4-n_3)/N^2$. The zero-field phase diagram is presented in Fig. 1, where the phase transitions take place along the curves a, b, and c. Several aspects of the phase diagram are unusual, i.e., the ordered states (both ferroelectric and antiferroelectric) are frozen-in zero-entropy phases and the disordered phase of the symmetric six-vertex model is replaced by a ferrielectric phase, with large entropy, but nonvanishing polarizations.

The exact solution can also be obtained in the presence of a field ($\omega_4 \neq \omega_3$) [14]: in this case the Boltzmann weights are four, corresponding to three independent parameters. This generalization is important for the application to surfaces, which is the main concern of this paper.

Using the five-vertex representation, we calculate in the following section the mean square height difference (MSHD) of the surfaces studied. With the knowledge of the value of the MSHD we can classify the surfaces, corresponding to different phases of the five-vertex model, into smooth and rough surfaces. If no field is applied, the flat surfaces undergo a transition at a critical temperature, where the inclination of the surfaces changes, and they become rough. If, however, the inclination is kept constant by applying a suitable field, the flat surfaces remain smooth from zero up to infinite temperature, without undergoing any roughening transition.

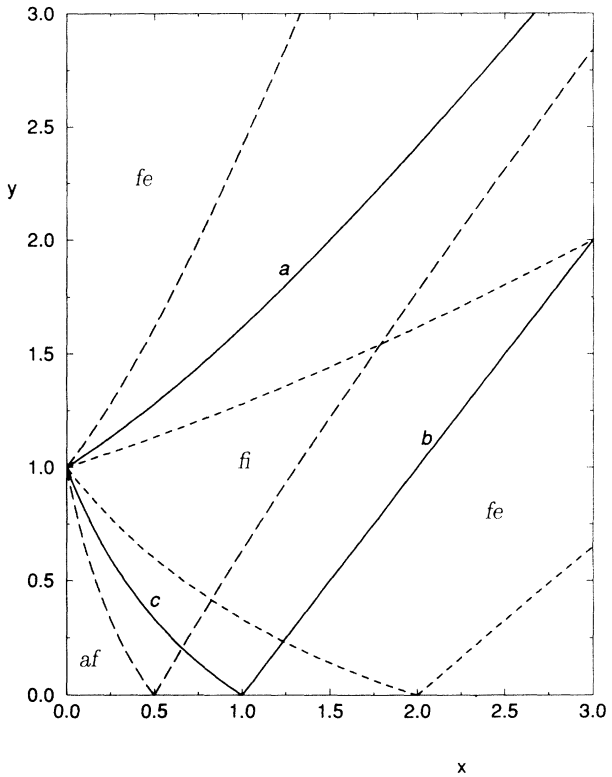

FIG. 1. The phase diagram of the five-vertex model in an external field, in terms of the Boltzmann weights $x = \omega_1/\omega_5$ and $y = \omega_3/\omega_5$ ($\omega_2 = 0$, $\omega_3 = \omega_4$, and $\omega_5 = \omega_6$), for three constant values of V: V = 0.5 (short-dashed line), $V = 1.0$ (continuous line), and $V = 2.0$ (long-dashed line). All curves represent second-order transitions. The a, b, and c curves represent the phase diagram in zero external field $V = 1$. fe stands for a ferroelectric, fi for a ferrielectric, and af for an antiferroelectric phase. The $x = y = 1$ point corresponds to infinite temperature, while any point satisfying $x/y = 0$ or $y/x = 0$ corresponds to a zero-temperature state.

II. THE MEAN SQUARE HEIGHT DIFFERENCE

The mean square height difference over the interface is

$$g_{ij} = \langle [m_{ij} - m_{00}]^2 \rangle , \tag{3}$$

where $m_{ij} = m(\mathbf{R}_{ij})$ is the surface level (meaured in crystal spacings) at site $\mathbf{R}_{ij}$ on the surface, g_{ij} depends asymptotically only on the distance $R \equiv |\mathbf{R}_{ij} - \mathbf{R}_{00}|$ and the ensemble average is taken for the SOS system. The behavior of g_{ij} defines roughness: if the asymptotic value of g_{ij} is finite, the interface is smooth; if it is infinite, the interface is rough. Hereafter, we calculate exactly the mean square height difference along a row, i.e., we extract

$$g_j = g_{0j} = \langle [m_{0j} - m_{00}]^2 \rangle , \tag{4}$$

in the exactly solvable five-vertex model.

In the GLT mapping scheme, as presented in Sec. I, the mean inclination of a facet corresponds to $P_v = (n_3 + n_5)/N$ and $P_h = (n_4 + n_5)/N$. Here n_i is the number of vertices i in a row of the corresponding five-vertex model. Using the definition [11] of the vertical and horizontal polarizations of the five-vertex model, i.e., $p_v = (n_1 + n_4 - n_3)/N$ and $p_h = (n_1 + n_3 - n_4)/N$, the results

$$P_v = \frac{1 - p_v}{2} , \; P_h = \frac{1 - p_h}{2} \tag{5}$$

are immediately obtained. [We should mention that, similarly, in the body-centered SOS (BCSOS) mapping the surface inclination is given by the vertical and horizontal polarizations of the corresponding six-vertex model.]

Considering the phase diagram of the five-vertex model and using the simple Eqs. (5) it can be seen that the frozen-in ferroelectric phase correspond to the smooth surfaces of the sc crystal. More specific, the Fe I phase corresponds [8] to the (100) surface and the Fe II phase to the (110) surface of a sc crystal.

Returning to the MSHD, for the five-vertex case the height difference which gives an inclination equal to P_v is

$$m_{0j} - m_{00} = \sum_{j'}^{j} \frac{1 - \sigma_{j'}}{2} , \tag{6}$$

where $\sigma_j = \pm 1$ is the vertical arrow variable at link j along the horizontal row. The MSHD in a row defined in Eq. (4) becomes

$$g_j = \frac{1}{4} j + \frac{1}{2} \sum_{l=1}^{j-1} (j - l) \langle \sigma_0 \sigma_l \rangle . \tag{7}$$

Only the asymptotic behavior of g_j is relevant for criticality. Thus we are led to look for the asymptotic behavior of the $\langle \sigma_0 \sigma_l \rangle$ equal-time correlation function. This can be determined [15] using the results of the quantum inverse scattering method [16], which are generally valid for integrable models and can be applied directly to the vertex model or indirectly to its quantum spin chain transform [17]. Thus we use the result [16],

$$\langle \sigma_0 \sigma_l \rangle = -\frac{K}{l^2} + (-1)^l K' \frac{\cos(\pi l p_v)}{l^\theta} . \tag{8}$$

In the region of the phase diagram close to the smooth surfaces (see Fig. 1) $p_v \to 1$ (we are approaching the ferroelectric phases), the critical exponent is $\theta = 2$ and $K = -K'$. Both terms of Eq. (8) contribute to the MSHD, and Eq. (7) gives

$$g_j = K \ln j , \tag{9}$$

where K is the corresponding roughness constant.

Thus the fi phase of the five-vertex model (see Fig. 1) corresponds to a rough surface of a sc crystal. Since this domain corresponds to a ferrielectric phase, it has nonvanishing polarization; the corresponding vicinal surface will exhibit rounded edges for vicinal areas.

III. SURFACE BEHAVIOR IN THE FIELD-FREE GLT MAPPING

Let us consider once more the phase diagram of Fig. 1, and focus attention on a particular choice of parameters in the Hamiltonian, namely, $\varepsilon_1 < \varepsilon_3 = \varepsilon_5$ ($\varepsilon = \varepsilon_5 - \varepsilon_1$). This is a particularly easy, *free fermion* case whose partition functions was found many years ago by Wu [18]. More recently Garrod was able to calculate two- and three-point correlations for this case [10]. It corresponds to moving, as a function of temperature, on the horizontal straight-line trajectory $y \equiv 1$, from $x = \infty$ ($T = 0$) to $x = 1$ ($T \to \infty$). For $x > 2$ ($kT < kT_c = \varepsilon / ln\ 2$) we have a trivial frozen, ideal, flat (100) surface. All vertices are of type 1: there are no defects, no entropy, and no fluctuations. At $x = 2$ a second-order phase transition, of the Pokrovsky-Talapov type [19], takes place, and steps appear spontaneously, with a density $\sim (2 - x)^{1/2}$; for details see Sec. VI.

The surface turns, therefore, to a vicinal, of general Miller indices (h, k, k), with $h >> k$. On the average, the steps have a kinematic kink every second site. Additional kinks and antikinks determine thermal meandering. In turn, this drives an overall thermal roughening of the vicinal surface. This seems to be a good realization, in an exactly solvable model, of the vicinal surface roughening described by Villain *et al.* [20]. At $x = 2$ the roughness parameter K jumps from zero to $2/\pi^2$.

As the temperature increases further, the step density increases continuously and so does the vicinal tilt angle $\theta = \arctan(\sqrt{2}k/h)$, tending ultimately to the $T \to \infty$ values $h = k$, $\theta = \arctan\sqrt{2}$. At $T = \infty$, the average orientation of the initially (100) surface is therefore (111). The surface is rough, but remarkably the roughness parameter K retains the constant value $K = 2/\pi^2$ at all temperatures $T > T_c$.

The above discussion refers to the $y \equiv 1$ case, but a very similar evolution occurs along more general trajectories (only the mathematics is more complicated because the free-fermion simplifications cannot be applied). In all cases, when starting from a flat surface at large x, the surface remains ideally (and trivially) flat up to the

phase boundary at $x - y = 1$; then it roughens, with a Pokrovsky-Talapov transition, and at the same time it begins to tilt, approaching progressively the (111) orientation. For the general case, using conformal field theory [16], for the roughness coefficient K is obtained

$$K = \frac{2}{\pi^2}\left[1 + P_v \frac{\Delta_5}{1-\Delta_5}\right] , \tag{10}$$

where Δ_5 and P_v are defined by Eqs. (1) and (5), respectively.

IV. THE PHASE DIAGRAM IN A FIELD

As we have just seen, the surface phase diagram in the field-free five-vertex model exhibits a T-dependent change of average orientation. While this might turn out to be of interest for special cases, it does represent a disturbing feature in a more conventional context, where the mean orientation is fixed by the boundary conditions.

Since the tilt angle corresponds simply to a finite polarization, it can be modified, and even suppressed, by the application of an external field. It is therefore quite fortunate that the five-vertex model can be solved exactly for an arbitrary field direction and intensity. We sketch the solution here; more details are contained in Ref. [14].

The arrow-reversal symmetry is already broken in the system by construction. Thus we expect that a direct external field will not change the behavior of the model. We could in principle apply a vertical (v) and a horizontal (h) field on every site. In fact, however, the physics of the five-vertex model only depends on the difference $h-v$ (changing the sum $h+v$ is in fact equivalent to changing the energy ε_1 of vertex 1). Thus it is not essentially restrictive to take $h = 0$. Rather than incorporating the vertical field into the vertex energies, let us keep ω_1, $\omega_3 = \omega_4$, and $\omega_5 = \omega_6$. In the noninteracting case, i.e., $y = 1$, the free energy becomes

$$f_L = \varepsilon_1 - v - k_B T \frac{q'}{\pi} \ln V + \frac{k_B T}{4\pi}\int_{-q'}^{+q'} \ln(x^2 + 1 - 2x\cos k)dk , \tag{11}$$

where $V = \exp(2v/k_BT)$. The integration limit is $q' = \arccos[(x^2+1-V^2)/(2x)]$. Two continuous phase transitions appear for $x = 1+V$ and $x = 1-V$ with critical exponent $\alpha = 1/2$. That is, the specific heat $c[T \to T_{c(+)}] \sim (T - T_c)^{-1/2}$, and it turns out that also the susceptibility has the same behavior in both cases.

This means that the critical exponent of the susceptibility is $\gamma = 1/2$. The vertical (p_v) and horizontal (p_h) polarizations per vertex can be easily computed, obtaining

$$p_v = 1 - \frac{2}{\pi}q' , \qquad p_h = 1 + \frac{2}{\pi}\arctan\left(\frac{\sin q'}{\cos q' - x}\right) . \tag{12}$$

It follows from Eq. (12) that in zero field the polarization per vertex is $p_v = p_h = 1 - (2/\pi)\arccos(x/2)$, identical with that obtained previously. Both p_v and p_h approach unity in both $x = 1 - V$ and $x = 1 + V$ transitions with a deviation proportional to $\sqrt{T - T_c}$.

Away from the free-fermion line ($\Delta_5 \neq 0$) we use the same method as in Ref. [11]. The transition curves (see Fig. 1) can be easily obtained with the use of the Legendre transform $f_L(v) = f_L(v=0) - vp_v$. Curves a, b, and c from Fig. 1, corresponding to zero external field, are transformed to

$$x = \frac{1}{V}\left(y - \frac{1}{y}\right) , \tag{13}$$

corresponding to curve a,

$$x = \frac{y}{2}(1+V) + [y^2(1-V)^2/4 + V^2]^{1/2} , \tag{14}$$

corresponding to curve b, and

$$x = V\frac{1-y}{1+y} , \tag{15}$$

corresponding to curve c, respectively. The phase transitions remain of the continuous type, with critical ex-

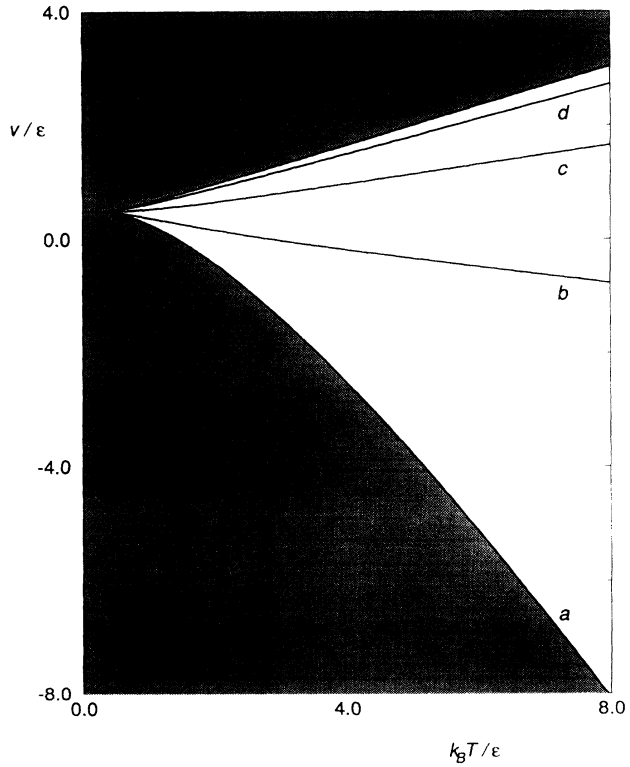

FIG. 2. The phase diagram of the modified KDP (potassium dihydrogen phosphate) model in an external field. The modified KDP model is defined by the energies $\varepsilon_1 = 0$, $\varepsilon_2 = \infty$, and $\varepsilon_3 = \varepsilon_4 = \varepsilon_5 = \varepsilon_6 = \varepsilon$. The continuous curves correspond to constant values of the vertical polarization: curve a, $p_v = 1$; curve b, $p_v = 1/2$; curve c, $p_v = 0$; curve d, $p_v = -1/2$; and curve e, $p_v = -1$. The shaded regions are ferroelectric phases, where the polarization is frozen into $p_v = 1$ or $p_v = -1$.

ponents $\alpha = 1/2$ and $\gamma = 1/2$, that is, both the specific heat and the susceptibility diverge like $(T-T_c)^{-1/2}$. The phase diagram for zero field and for different values of the external field is given in Fig. 2.

Note that the curves defined by Eq. (15) for any V and $x = 0$ give the only solution $y = 1$, while the curves given by Eqs. (13) and (14) intersect for any V at $y = 0$ and $x = V$; see Fig. 2. The system in all the three ordered phases exhibits a frozen-in state even in the presence of the external field.

V. SMOOTH VERSUS ROUGH SURFACES AT FIXED ORIENTATION

As we have shown in Sec. II, if we consider the GLT mapping, it is clear that we can interpret the polarizations P_v and P_h of the five-vertex model as height differences per unit length, yielding the surface slope. Thus, as in the case of the BCSOS model, we can directly translate the calculated quantities of the five-vertex model into the corresponding quantities of the GLT model. The only difference between the correspondences of models (six-vertex with BCSOS and five-vertex with GLT) is that for the latter p_v and p_h must be replaced by P_v and P_h.

Microscopically the roughening transition will be characterized by the emergence of strong height fluctuations on the facets. We are mainly interested in the fe I and fe II phases of Fig. 1, as they are appropriate for the GLT model. However, as we will see later, the c transition curve behaves similarly to the a or b curves.

The fe I phase from Fig. 1 is a frozen-in ferroelectric phase, whose free energy is equal to ε_1. Via the GLT mapping, this phase corresponds to a (100) surface of a sc crystal, as $P_v = 0$ and $P_h = 0$. The transition temperature at $V = 1$, see Eq. (14), is given by $y = x-1$, i.e.,

$$\exp\left(\frac{\varepsilon_5 - \varepsilon_4}{k_B T_c}\right) = 1 + \exp\left(\frac{\varepsilon_5 - \varepsilon_1}{k_B T_c}\right), \tag{16}$$

where $\varepsilon_3 = \varepsilon_4$ and $\varepsilon_5 = \varepsilon_6$. We are interested to know whether the surface (100) exhibits a roughening transition or not. For this purpose, we include an external field, imposing V to be such that the (100) inclination of the surface is kept constant (as we have seen, if no external field is applied, the inclination begins to vary with temperature at T_c). First let us consider the noninteracting $y = 1$ case. The values of V for which p_v and p_h are constants are easily obtained. The phase diagram versus the temperature is given in Fig. 2. Note that the $p_v = 0$ phase, existing in the case of the six-vertex model, shrinks to a point. As it can be seen from Eq. (12), fixing the polarizations at a constant value, we also fix the value of q'. However, the transition is given by the $q' = 0$ condition. Thus, fixing q' at a nonzero value the transition, corresponding to curve b, will not appear. This means that for $V = x - 1$ or $p_v = 1$, the system is built up by vertices of type 1 only and therefore that the (100) surface is smooth and frozen from $T = 0$ up to infinite temperature. On the other hand, for any value of V for which $p_v < 1$ and is constant, the corresponding surface is rough from $T = 0$ up to infinite temperature. The roughness constant K, see Eq. (9), does not vary with the temperature, being $K = 2/\pi^2$ through the whole temperature range.

Away from the noninteracting case, the situation is essentially the same. An external field which varies as

$$V = \frac{x(x-y)}{\sqrt{(y^2-1)(y^2-2xy-1)+x^2y^2}} \tag{17}$$

causes the integration limit Q from Eq. (1) to vanish and fixes the polarizations at the $p_v = p_h = 1$ values. Thus the free energy will be $f_L = \varepsilon_1 - v$ and the system will exhibit a frozen-in ferroelectric phase. As a consequence, the corresponding (100) surface will be smooth at any temperature. Fixing the polarizations at any other constant value $p_v \neq 1$, the corresponding surface will be rough at any temperature.

The af phase is not easily reached in the GLT mapping scheme. However, from the previous example we can see that in this case also, any external field which fixes the polarization fixes in the same manner the transition curve, given in Eq. (15), and the roughening transition shifts to $T \to \infty$.

The second frozen-in ferroelectric phase present in the phase diagram from Fig. 1 is the fe II phase. The fe II phase is built up with vertices 4 (or 3, since there is symmetry breaking in this case). This phase corresponds via the GLT mapping to a (110) surface of a sc crystal, as $P_v = 0$ and $P_h = 1$. [The case of vertex 3 would correspond to a $(\bar{1}01)$ surface, with $P_v = 1$ and $P_h = 0$.] The transition temperature for zero external field, see Eq. (14), is given by $x = y - 1/y$, i.e.,

$$\exp\left(\frac{\varepsilon_5 - \varepsilon_1}{k_B T_c}\right) = \exp\left(\frac{\varepsilon_5 - \varepsilon_4}{k_B T_c}\right) - \exp\left(\frac{\varepsilon_4 - \varepsilon_5}{k_B T_c}\right). \tag{18}$$

The (110) surface corresponding to the fe II phase is a perfectly smooth surface. The situation is analogous to the previous (100) case. That is, as the surface becomes rough, its inclination in zero field changes. With an appropriate external field we can fix the polarization and the transition is shifted away to infinite temperature. Thus we can conclude that also in this case the interface corresponding to the fe II phase is smooth from $T = 0$ up to infinite temperature.

VI. VICINAL AREAS

Flat facets and curved surface regions, when they meet at edges, can exhibit two types of behavior: sharp edges with slope discontinuity or (rounded) smooth edges with no slope discontinuity. Sharp edges correspond to first order, smooth edges to second order phase transitions [4,21,22].

As presented in Sec. IV the phase transitions exhibited by the five-vertex model in the presence of an external field are all continuous second order phase transitions. Thus, in the cases analyzed hereafter only smooth edges

can be found.

The behavior, near smooth edges, of the shape of the curved interface is critical. Thus it can be given in the form [16,23]

$$z - z_0 = \text{const} \times (x - x_0)^{\alpha} , \tag{19}$$

where α is a critical exponent. In order to calculate α we are looking for an expansion of the free energy of the form

$$f_L = f_L(P_v = 0) + P_v\, f_L^{[s]} + P_v^2\, f_L^{[2]} + P_v^3\, f_L^{[3]} + \cdots , \tag{20}$$

where $f_L^{[s]}$ represents the step free energy, the quadratic and higher-order terms arise due to step-step interaction.

Since the calculation procedure is rather involved, we describe it in detail only for the noninteracting fermion case. For the general case we give just the final results, restricting ourselves to a brief outline of the method used (see the Appendix).

In the noninteracting ($y = 1$) case we place ourselves near the b transition line (see Fig. 1), where the transition occurs at $x_c = 1 + V$, as determined in Sec. IV, with $V = 1$ corresponding to the zero-field case. On the $y = 1$ line, an expansion can be made from two directions. One is the $T > T_c$, i.e., $x < x_c$, case: the transition is approached from the rough side. We expand the expression of the free energy for the noninteracting case, given in Eq. (11) of Sec. IV, in Taylor series as a function of P_v, around $P_v = 0$, and using $\partial/\partial P_v \equiv (\partial x/\partial P_v)\, \partial/\partial x$ we obtain

$$f_L = f_L(P_v = 0) + k_B T_c\, f_L^{[2]}(x_c, y = 1, V)\, P_v^2 + \cdots , \tag{21}$$

where $f_L^{[2]}(x_c, y = 1, V) = 2\pi^2 x_c^2/[(x_c - 1)(x_c^2 - 1 + V^2)]$, which reduces to $f_L^{[2]}(x_c, y = 1, 1) = \pi^2$ in the zero external field limit. Comparing Eq. (21) to Eq. (20) it can be seen that the linear term $f_L^{[s]}$ is missing from Eq. (21). Thus the step free energy is zero, as required for a rough surface.

In order to see the critical behavior at smooth edges the expansion from Eq. (20) must be done from the smooth side. That is, we are looking for an expansion in the $T < T_c$ or $x > x_c$ limit. This amounts to perturb the smooth, frozen-in surface by introducing a small step density [given by a small P_v, in the form $q' = \pi P_v \ll 1$; see Eq. (11)] and computing the effect on the free energy. Contrary to the previous ($T > T_c$) case, in the present situation P_v is independent of x. (P_v in this case is a small perturbation introduced artificially to perturb the smooth surface.) Thus we need to perform a two-variable Taylor expansion, in both variables x and P_v, around $x = x_c$ and $P_v = 0$. In order to do this, we write the expression of the free energy from Eq. (11) with the use of Clausen's integral

$$\mathrm{Cl}_2(x) = -\int_0^x \ln[2\sin(x'/2)]dx', \tag{22}$$

obtaining

$$f_L = \varepsilon_1 - v - k_B T\, P_v\, \ln V + \frac{k_B T}{2\pi}[\mathrm{Cl}_2(2\pi P_v + 2\eta) - \mathrm{Cl}_2(2\pi P_v) - \mathrm{Cl}_2(2\eta) - 2\eta \ln x] , \tag{23}$$

where $\eta = \tan^{-1}\{\sin(\pi P_v)/[1/x - \cos(\pi P_v)]\}$. Close to the transition, using the expansion [24] of Clausen's integrals for small argument, the free energy from the above equation becomes

$$f_L = \varepsilon_1 - v - k_B T_c\, P_v\, \ln V + \frac{k_B T_c}{\pi}\, \ln x_c\, \tan^{-1} \frac{\sin(\pi P_v)}{\cos(\pi P_v) - 1/x_c} . \tag{24}$$

Expanding in powers of P_v, we obtain

$$f_L = f_L(P_v = 0) + k_B T_c\, f_L^{[s]}(x_c, y = 1, V)\, P_v - k_B T_c\, f_L^{[3]}(x_c, y = 1, V)\, P_v^3 + \cdots , \tag{25}$$

where $f_L^{[s]}(x_c, y = 1, V) = [x_c/(x_c - 1)] \ln x_c - \ln V$ and $f_L^{[3]}(x_c, y = 1, V) = (\pi^2/6)[x_c(x_c + 1)/(x_c - 1)^3] \ln x_c$. In the free field case, these coefficients reduces to $f_L^{[s]}(x_c, y_c = 1, 1) = 2 \ln 2$ and $f_L^{[3]}(x_c, y_c = 1, 1) = \pi^2 \ln 2$.

Away from the noninteracting case, we have two transitions to analyze, corresponding to curves a and b of Fig. 1. We borrow the calculation method from the noninteracting case; the calculations are given in the Appendix.

The results are rather simple: Eq. (A10) of the Appendix can be reduced to a form of Eq. (19),

$$Z - Z_0 = \frac{2}{3^{3/2}}\, (f_L^{a,b\,[3]})^{-1/2}\, (X - X_0)^{3/2} , \tag{26}$$

where the coefficient of Eq. (26) reduces to $2\pi/[9(\varepsilon_5 - \varepsilon_1)^{1/2}]$ in the noninteracting limit. Equation (26) defines nothing else than the Pokrovsky-Talapov [19] or Gruber-Mullins [25] universality class.

Another intereseting quantity is the distribution of terrace widths. The surface mapping procedure used throughout the present analysis assumed that steps do not cross each other; there are no overhangs and neither step terminates. In these conditions, there is no significant energetic intercations between steps (except entropic repulsion); thus their structural properties can be described [26] in terms of two lengths: (i) the average length along the direction of step wandering between close approaches of adjacent steps and (ii) the average spacing between steps $\langle L \rangle$. These spacings are in the direction perpendicular to the average direction along which the step edge runs. As the energetic intercations are insignificant, there is no competing length in this direction; thus $\langle L \rangle$ is determined solely by the vicinal tilt (or misorientation [26]) angle θ (for a definition, see Sec. III). As in our model there are only single height steps, the density of steps is $1/\langle L \rangle = \tanh\theta$ and is largely independent of temperature [26].

In the GLT mapping scheme, as demonstrated in

Sec. II, the mean inclination of a facet, i.e., $\tanh\theta$, corresponds to P_v defined in Eq. (5). This quantity can be easily calculated from the expression of the free energy close to the transitions, i.e., curves a and b of Fig. 1. The free energy close to these transtion curves is given by Eq. (A1) for curve a and by Eq. (A2) for curve b, respectively. We approach these transition curves from the rough surface on a $y = \text{const}$ line. The transitions ooccur at $x = x_c$, with x_c given in Eq. (13) for the a transition curve and in Eq. (14) for the b curve. Performing a generalized series expansion of P_v for $x \to x_c$, we obtain for the density of steps

$$\frac{1}{L} \sim \sqrt{\frac{2}{x_c}}\sqrt{x_c - x}\,. \tag{27}$$

That is, in a Pokrovsky-Talapov transition the steps appear spontaneously with a density proportional to $\sqrt{x_c - x}$.

VII. DISCUSSION AND CONCLUSIONS

One of the simplest ways to model the crystal-vapor interface is to consider densely packed atoms sitting on top of each other, without vacancies or overhangs. Fortunately, some versions of the so defined SOS model are isomorphic to exactly solvable two-dimensional statistical mechanics models, so that the behavior of the interfaces, however unusual, can be predicted exactly. The most frequently used mapping scheme is that of van Beijeren [3], establishing a correspondence between some surfaces of well-defined crystals and the six-vertex model [6,7]. This mapping is suitable for lattices which are naturally separable into two sublattices, that is, surfaces of bipartite lattice structure. Due to this, the BCSOS mapping scheme worked well in cases such as the (001) facet [3] of a bcc crystal or the (001) and (011) facets [4,5] of an fcc crystal.

For other surfaces, e.g., for the (100) surface of the sc crystal, however, this is not the case: the two-dimensional lattice structures do not split naturally into two sublattices. In this case the GLT [8] mapping scheme can be used: then the corresponding statistical-mechanical problem generates a five-vertex model. Using the exact solution of the five-vertex model [11] we were able to show that the frozen-in ferroelectric phases and the ferrielectric phase that appear in the solution of the five-vertex model (see Fig. 1) are suitable for the GLT mapping. The fe I phase correponds to the (100) surface of a sc crystal and the fe II phase to the (110) or the $(\bar{1}01)$ surface of a sc crystal. These interfaces are flat and completely smooth. As we move away from the fe I or fe II phases into the fi phase the curvature of the surfaces changes smoothly and the interface becomes rough. The roughness coefficient K, calculated for the noninteracting case, shows no temperature dependence up to infinitely high temperatures. Due to this behavior, the five-vertex model is most suitable to describe the rounded facet edges (corresponding to vicinal areas), as shown in Sec. VI.

To study the possible roughening transitions, we must fix the inclination of the surface. This is done in the five-vertex model with the introduction of an external field. In Sec. IV, the properties of the five-vertex model in the presence of an external field are briefly presented and the phase diagram is established. With these results we were able to establish that the (100), (110), and $(\bar{1}01)$ flat surfaces of a sc crystal remain smooth from $T = 0$ up to infinite temperature. However, when an infinitesimal but nonvanishing and constant inclination is applied to these surfaces, the corresponding vicinal surfaces are rough from $T = 0$ up to infinite temperature. In either case, these surfaces do not therefore undergo any finite-temperature roughening transition.

In Sec. VI the rounded portions of the equilibrium shape have been considered. Their properties are determined by both the step energy and the step interactions. Since two steps at a distance d from each other have an interaction energy proportional to d^{-2} (repulsive if the two steps have the same sign, attractive if they have opposite signs), the form of the rounded portions is conventional, i.e., the coordinates x and z are connected to each other as

$$z - z_0 \sim -(x - x_0)^{\theta},$$

with $\theta = 3/2$, in accordance with the treatments of Gruber and Mullins [25] and Pokrovsky and Talapov [19] (the same held for the six-vertex model in van Beijeren's mapping, as shown by Nolden [22]).

APPENDIX: EXPANSIONS OF THE FREE ENERGY

In the interacting case we have two transitions to analyze, curves a and b of Fig. 1. We approach the transition curves from a rough surface on a $y = \text{const}$ line. The free energy close to the transition curves, see Eq. (1) and Refs. [11,14], is equal to

$$f_L^a = \varepsilon_4 - v + k_BT\frac{q'}{\pi}\ln\left(\frac{y}{V}\right) + \frac{k_BT}{2\pi}\int_0^{q'}\ln(x^2 + y^2 - 2xy\cos k)\,dk \tag{A1}$$

near the a transition curve and

$$f_L^b = \varepsilon_1 - v + k_BT\frac{q'}{\pi}\ln\left(\frac{x}{V}\right) - \frac{k_BT}{2\pi}\int_0^{q'}\ln\left(y^2 + \frac{1 - 2y^2 + 2xy\cos k}{x^2 + y^2 - 2xy\cos k}\right)dk \tag{A2}$$

near the b transition curve, respectively. An expansion of Eqs. (A1) and (A2) gives a behavior of the free energy identical to Eq. (21) with

$$f_L^{a\,[2]}(x_c, y, V) = 2\pi^2\frac{x_c^3 y}{(x_c - y)(x_c^2 - y^2 + V^2/y^2)} \tag{A3}$$

for the a transition curve, where x_c is given in Eq. (13) and

$$f_L^{b\,[2]}(x_c,y,V) = \frac{2x_c^2yV^4\pi^2}{x_c-1}\,(1-y^2+x_c^2/V^2)\,[x_c + (x_c-1)(1-y)] \times \{x_c^4(x_c^2-y^2)+x_c^2V^2(y^2-x_c^2-1)(2y^2-3)-V^4(y^2-1)[(y^2-1)^2-x_c^2y^2]\}^{-1} \tag{A4}$$

for the b transition curve, with x_c given in Eq. (14).

To see the critical behavior at the smooth edges along both transition curves we write Eqs. (A1) and (A2) in the form

$$f_L^a = \varepsilon_4 - v + k_BT\,\frac{q'}{\pi}\,\ln\left(\frac{y^2}{V}\right) + \frac{k_BT}{2\pi}\left[\mathrm{Cl}_2(2\pi P_v+2\eta)-\mathrm{Cl}_2(2\pi P_v) -\mathrm{Cl}_2(2\eta)-2\eta\ln\left(\frac{x}{y}\right)\right], \tag{A5}$$

for curve a and

$$f_L^b = \varepsilon_1 - v - k_BT\,\frac{q'}{\pi}\,\ln V + \frac{k_BT}{2\pi}\left[\mathrm{Cl}_2(2\pi P_v+2\eta)-\mathrm{Cl}_2(2\pi P_v+2\eta') -\mathrm{Cl}_2(2\eta)+\mathrm{Cl}_2(2\eta') - 2\eta\ln\left(\frac{x}{y}\right)+2\eta'\ln\left(\frac{y^2-1}{xy}\right)\right] \tag{A6}$$

for curve b, respectively, where $\mathrm{Cl}_2(x)$ is Clausen's integral (21), $\eta=\tan^{-1}\{\sin(\pi P_v)/[y/x-\cos(\pi P_v)]\}$, and $\eta'=\tan^{-1}\{\sin(\pi P_v)/[xy/(y^2-1)-\cos(\pi P_v)]\}$.

From Eqs. (A5) and (A6) we immediately obtain for the free energy close to the transition curves the form known from the noninteracting limit; see Eq. (25):

$$f_L^{a,b} = f_L^{a,b}(P_v=0)+k_BT_cf_L^{a,b\,[s]}(x_c,y,V)P_v -k_BT_c\,f_L^{a,b\,[3]}(x_c,y,V)\,P_v^3+\cdots, \tag{A7}$$

where

$$f_L^{a\,[s]}(x_c,y,V)=\frac{x_c}{x_c-y}\ln\left(\frac{x_c}{y}\right)-\ln V+2\ln y, \tag{A8}$$

$$f_L^{a[3]}(x_c,y,V)=\frac{\pi^2}{6}\frac{x_cy(x_c+y)}{(x_c-y)^3}\ln\left(\frac{x_c}{y}\right),$$

and

$$f_L^{b[s]}(x_c,y,V)=\frac{x_c}{x_c-y}\ln(\frac{x_c}{y})-\ln V -\frac{y^2-1}{y^2-xy-1}\ln\left(\frac{y^2-1}{xy}\right), \tag{A9}$$

$$f_L^{b\,[3]}(x_c,y,V)=\frac{\pi^2}{6}\frac{x_cy(x_c+y)}{(x_c-y)^3}\ln\left(\frac{x_c}{y}\right) -\frac{\pi^2}{6}\,x_cy(y^2-1) \times\frac{y^2+x_cy-1}{(y^2-x_cy-1)^3}\ln\left(\frac{y^2-1}{xy}\right).$$

Using the expression of the crystal shape in the (X,Y,Z) plane from the Wulff construction [22] with the obvious change $p_v\to P_v$ we obtain from Eq. (A7)

$$Z = Z_0+2k_BT_cf_L^{a,b\,[3]}P_v^3, \qquad X = X_0+3k_bT_cf_L^{a,b\,[3]}P_v^2. \tag{A10}$$

[1] W. K. Burton and N. Cabrera, Disc. Faraday Soc. **5**, 40 (1949); W. K. Burton, N. Cabrera, and F. C. Frank, Philos. Trans. R. Soc. London Ser. A **243**, 299 (1951).

[2] E. H. Hauge and P. C. Hemmer, Phys. Norv. **5**, 209 (1974); C. Deutsch and M. Lavaud, Phys. Rev. A **9**, 2598 (1974).

[3] H. van Beijeren, Phys. Rev. Lett. **38**, 993 (1977).

[4] C. Jayaprakash and W. F. Saam, Phys. Rev. B **30**, 3917 (1984); C. Jayaprakash, C. Rottman, and W. F. Saam, *ibid.* **30**, 6549 (1984).

[5] A. Trayanov, A. C. Levi, and E. Tosatti, Surf. Sci. **233**, 184 (1990).

[6] E. H. Lieb and F. Y. Wu, in *Phase Transition and Critical Phenomena*, edited by C. Domb and M. S. Green (Academic, London, 1972), Vol. 1.

[7] R. J. Baxter, *Exactly Solvable Models in Statistical Physics* (Academic, London, 1982).

[8] C. Garrod, A. C. Levi, and M. Touzani, Solid State Commun. **75**, 375 (1990).

[9] C. Garrod, Phys. Rev. A **41**, 4184 (1990).

[10] C. Garrod, J. Stat. Phys. **63**, 987 (1991).

[11] M. Gulácsi, H. van Beijeren, and A. C. Levi, Phys. Rev. E **47**, 2473 (1993).

[12] The connection between the five-vertex and the asymmetric six-vertex models is discussed in details in Ref. [11].

[13] J. Dong and D. Kim, SNUTP Report No. 93-66, 1993 (unpublished).

[14] M. Gulácsi, Ph.D. thesis, Scuola Internazionale Superiore di Studi Avanzati, Trieste, 1991.

[15] The only ingredient needed for the technique, described in Ref. [16], to work is to have a low-energy linear spectrum. This requirement is satisfied for any integrable model for $p_v \le 1$.

[16] V. E. Korepin, Theor. Math. Phys. **41**, 953 (1979) [Teor. Mat. Fiz. **41**, 169 (1978)]; A. G. Izergin and V. E. Korepin, Commun. Math. Phys. **94**, 67 (1984); V. E. Korepin, *ibid.* **94**, 93 (1984); A. G. Izergin and V. E. Korepin, *ibid.*

99, 271 (1985); N. M. Bogoliubov, A. G. Izergin, and V. E. Korepin, Nucl. Phys. B **275**, 687 (1986).
[17] L.-H. Gwa and H. Spohn, Phys. Rev. A**46**, 844 (1992).
[18] F. Y. Wu, Phys. Rev. Lett. **22**, 1174 (1969); **24**, 1476 (1970).
[19] V. L. Pokrovsky and A. L. Talapov, Phys. Rev. Lett. **42**, 65 (1979).
[20] J. Villain, D. R. Grempel, and J. Lapujoulade, J. Phys. F **15**, 809 (1985).
[21] D. B. Abraham, in *Phase Transition and Critical Phenomena*, edited by C. Domb and J. L. Lebowitz (Academic, New York, 1986), Vol. 10; B. Nienhuis, in *ibid.* (Academic, New York 1987), Vol. 11.
[22] H. van Beijeren and I. Nolden, in *Structure and Dynamics of Surfaces II*, edited by W. Schommers and P. von Blanckenhagen, Topics in Current Physics, Vol. 43 (Springer, New York, 1987); I. Nolden, Ph.D. thesis, University of Utrecht, 1990.
[23] A. F. Andreev, Zh. Eksp. Teor. Fiz. **80**, 2042 (1981) [Sov. Phys. JETP **53**, 1063 (1981)].
[24] I. S. Gradshteyn and I. M. Ryzhik, *Tables of Integrals, Series and Products* (Academic, New York, 1980).
[25] E. E. Gruber and W. W. Mullins, J. Phys. Chem. Solids **28**, 875 (1967).
[26] B. Joós, T. L. Einstein, and N. C. Bartelt, Phys. Rev. B **43**, 8153 (1991).